JACS
JOURNAL OF THE AMERICAN CHEMICAL SOCIETY

Communication

Chiral Metallacycles as Catalysts for Asymmetric Conjugate Addition of Styrylboronic Acids to #,#-Enones

Tao Hong, Zibin Zhang, Yan Sun, Jia-Ju Tao, Jia-Dong Tang, Chunsong Xie, Min Wang, Fang Chen, Shang-Shu Xie, Shijun Li, and Peter J. Stang

J. Am. Chem. Soc., **Just Accepted Manuscript** • DOI: 10.1021/jacs.0c01563 • Publication Date (Web): 20 May 2020

Chiral Metallacycles as Catalysts for Asymmetric Conjugate Addition of Styrylboronic Acids to *α,β*-Enones

Tao Hong,[†] Zibin Zhang,[†] Yan Sun,[‡] Jia-Ju Tao,[†] Jia-Dong Tang,[†] Chunsong Xie,[†] Min Wang,[†] Fang Chen,[†] Shang-Shu Xie,[†] Shijun Li,[*,†] and Peter J. Stang[*,‡]

[†]College of Material, Chemistry and Chemical Engineering, Hangzhou Normal University, Hangzhou 311121, China

[‡]Department of Chemistry, University of Utah, 315 South 1400 East, Room 2020, Salt Lake City, Utah 84112

Supporting Information Placeholder

ABSTRACT: Introducing self-assembly strategies into the construction of catalysts has been proven to have great advantages in asymmetric catalysis. We constructed two chiral metalla-triangles by highly efficient coordination-driven self-assembly from a chiral 3,3'-dipyridyl substituted BINOL donor. They were successfully applied in asymmetric conjugate addition of a series of *α,β*-unsaturated ketones with *trans*-styrylboronic acids. The use of these metalla-triangles as supramolecular catalysts is obviously conducive to the enhancement of catalytic activity and stereoselectivity in the presented addition reactions. Under induction of the chiral metalla-triangles, an array of *α,β*-enones were converted to chiral *γ,δ*-unsaturated ketones in medium to quantitative yields (40–98%) with high enantioselectivities (87–96% ee).

In the past two decades, supramolecular catalysis has attracted growing attention due to the great advantages of introducing self-assembly strategies into the construction of catalysts.[1] The dynamic and reversible properties of supramolecular interactions make it much easier to fabricate enzyme-mimicking catalysts and to establish catalyst libraries, which are beneficial to the achievement of unexpected catalytic activity and selectivity.[2] A variety of artificial supramolecular catalysts have been prepared on basis of different recognition motifs,[1,2] such as host-guest complexations,[3] metal–ligand interactions,[1g,4] hydrogen bonds,[5] and hydrophobic effects.[6] However, there are only few examples of chiral supramolecular catalysts and an even smaller number have high stereoselectivity in the application of asymmetric catalysis.[2]

On the other hand, along with the rapid growth of coordination-driven self-assembly (CDSA), plenty of discrete metalla-supramolecules with well-defined shapes and sizes have been successfully prepared.[7] A wide range of metals and ligands have been utilized to form supramolecular coordination complexes (SCCs) that not only exhibited interesting topological structures but also showed numerous applications in chemical sensing,[8] host-guest chemisty,[9] crystalline sponges,[10] artificial light harvesting,[11] separation,[12] stimuli-responsive materials,[13] biomedicine,[14] and so on. The high efficiency of CDSA also enables it as a powerful method to construct chiral self-assemblies.[15,16] A few chiral platinum-based SCCs have been successively synthesized since the first report by Stang et al in 1996.[16a] Recently, a platinum-based chiral tetrahedral cage was synthesized and used to catalyze the Michael addition of nitrostyrene derivatives with indole.[16e] However, no enantioselectivity was observed because the chiral ligands of the cage locate at peripheral positions.[16e] We speculated that incorporation of a chiral catalyst into the center of a conformationally rigid metallacycle or metallacage would lead to an effective chiral supramolecular catalyst with a well-defined enzyme-like cavity. As the catalytic centers will be in a confined space of the cavity tightly surrounded by several chiral building blocks, it can be deduced that the induced asymmetric reaction will be better than that catalyzed by the non-assembled catalyst.

1,1'-Binaphthol (BINOL, **1**) has become a widely used chiral ligand since its first application in asymmetric reaction by Noyori et al in 1979.[17] In recent decades, numerous effective catalysts with the binaphthyl core structure have been successfully utilized in various asymmetric catalytic reactions,[18] especially with the 3,3'-position functionalized BINOL derivatives.[19,20] To test our hypothesis, we designed and synthesized chiral BINOL-incorporated metallacycles by using CDSA, and applied these metallacycles in catalyzing the asymmetric addition of styrylboronic acids to *α,β*-enones. Obvious enhancement of both activity and stereoselectivity was achieved when the chiral BINOL-incorporated metallacycles were used as the catalysts.

Scheme l. Synthesis of chiral BINOL derivative (*S*)-5 [a]

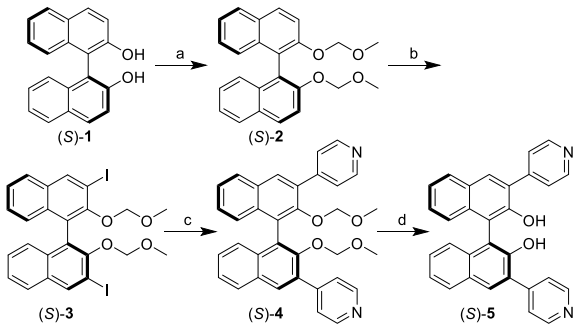

[a]Reagents and conditions: (a) NaH, chloromethyl methyl ether, THF, 90% yield; (b) I_2, *n*-BuLi THF, –78 ℃, 72% yield; (c) 4-pyridineboronic acid pinacol ester, $Pd_2(dba)_3$, K_3PO_4, tricyclohexyl phosphine, H_2O/1,4-dioxane, 100 ℃, 89% yield; (d) HCl, H_2O, 90% yield.

As shown in Scheme 1, a 3,3'-dipyridyl substituted chiral BINOL donor (*S*)-**5** was firstly synthesized from the commercially available (*S*)-BINOL **1** in four steps. After protection by chloromethyl methyl ether, (*S*)-**2** was iodinated to give 3,3'-diiodo-2,2'-bis(methoxymethoxy)-1,1'-binaphthalene (*S*)-**3** in 72%

yield. Suzuki cross-coupling of (*S*)-**3** with 4-pyridineboronic acid pinacol ester and deprotection in hydrochloric acid furnished the target bidentate BINOL donor (*S*)-**5** in 52% overall yield from (*S*)-BINOL **1**. The prepared (*S*)-**5** was proven enantiometrically pure by using chiral HPLC analysis (Figure S10).

Two component CDSA was then performed by stirring the ligand (*S*)-**5** with the 180 ° Pt-based acceptor **6a** or **6b** in 1:1 mole ratio to produce two homochiral metallacycles (*S*)-**7a** and (*S*)-**7b** in quantitative yields (Scheme 2). $^{31}P\{^{1}H\}$ and ^{1}H NMR spectroscopy of the self-assemblies supported the formation of single, discrete chiral metallacycles with highly symmetric structures (Figure 1 and 2). The $^{31}P\{^{1}H\}$ NMR spectra of both (*S*)-**7a** (Figure 1b and S14) and (*S*)-**7b** (Figure 1c and S19) displayed a single peak with two concomitant ^{195}Pt satellites, consistent with the homoligated Pt-N coordination environment. After formation of the two chiral metallacycles, the signals in $^{31}P\{^{1}H\}$ NMR spectra of (*S*)-**7a** and (S)-**7b** shifted upfield from those of the starting platinum acceptor **6a** and **6b** by approximately 5.52 ppm (Figure 1b *vs* 1a) and 5.65 ppm (Figure 1c *vs* 1d), respectively.

Scheme 2. Self-assembly of the chiral metalla-triangles (*S*)-7a and (*S*)-7b

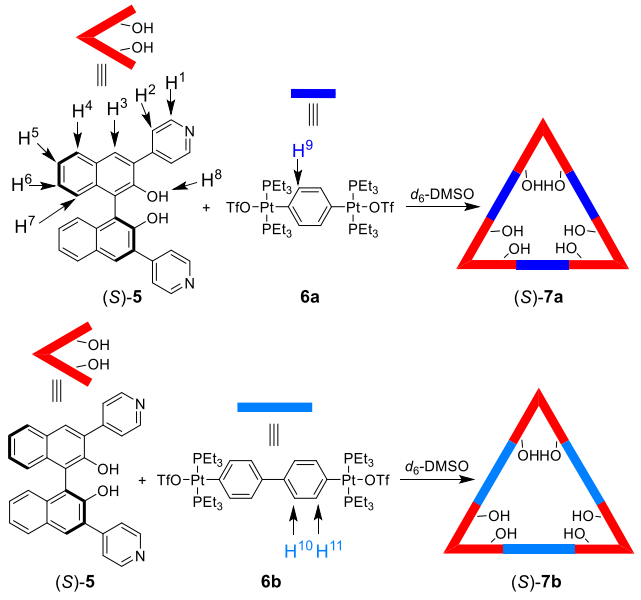

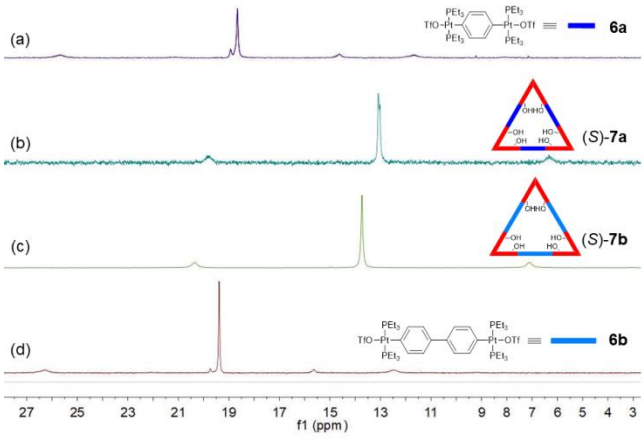

Figure 1. $^{31}P\{^{1}H\}$ NMR (202 MHz, d_6-DMSO, 22 ℃) spectra of (a) **6a**, (b) (*S*)-**7a**, (c) (*S*)-**7b**, and (d) **6b**.

By investigation of the ^{1}H–^{1}H COSY spectra of (*S*)-**7a** (Figure S13), (*S*)-**7b** (Figure S18) and (*S*)-**5** (Figure S6), all proton peaks were assigned clearly. Readily apparent shifts of the peaks found in the ^{1}H NMR spectra of (*S*)-**7a** (Figure 2b and S12) and (*S*)-**7b** (Figure 2d and S17) were also observed, as compared with their analogues in the ^{1}H NMR spectra of **6a** (Figure 2a), **6b** (Figure 2e), and (*S*)-**5** (Figure 2c), respectively. Upon the formation of (*S*)-**7a** and (*S*)-**7b**, not only the aromatic protons of (*S*)-**5** shifted downfield, especially the ones close to the platinum, like H^1, H^2 and H^3, but also the hydroxy proton H^8 shifted downfield significantly. Simultaneously, the signals for H^9 of **6a** and H^{10}, H^{11} of **6b** shifted downfield after the exchange of ligands. Circular dichroism (CD) explicitly affirmed the chirality of the metallacycles (*S*)-**7a** and (*S*)-**7b** (Figure S16 and S21).

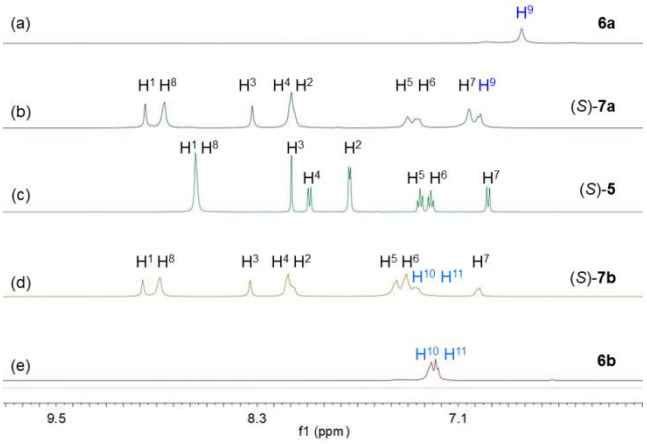

Figure 2. Partial ^{1}H NMR (500 MHz, d_6-DMSO, 22 ℃) spectra of (a) **6a**, (b) (*S*)-**7a**, (c) (*S*)-**5**, (d) (*S*)-**7b**, and (e) **6b**.

Table 1. Effects of additive and solvent on the asymmetric conjugate addition of chalcone 8a catalyzed by (*S*)-7a [a]

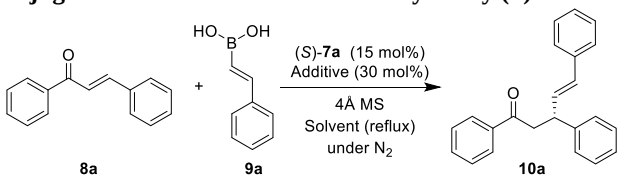

Entry	Additive	Solvent	Conv. (%) [b]	ee (%) [c]
1	$Mg(OtBu)_2$	CH_3CN	38	89
2	$Mg(OtBu)_2$	DMF	trace	n.d[d]
3	$Mg(OtBu)_2$	CH_2Cl_2	5	n.d[d]
4	$Mg(OtBu)_2$	Toluene	50	77
5	$MgSO_4$	CH_3CN	54	82
6	$MgCl_2$	CH_3CN	43	83
7	$MgBr_2$	CH_3CN	38	82
8	$Mg(OEt)_2$	CH_3CN	35	86

[a] Reaction conditions: 0.03 mmol **8a**, 0.036 mmol **9a**, 0.0045 mmol (*S*)-**7a**, concentration of **8a** = 0.05 M, 4Å MS (16 mg), reaction time = 40 h. [b] Determined by integration of product in ^{1}H NMR spectra. [c] Determined by HPLC analysis. [d] Not determined.

The self-assembly stoichiometry of the chiral metallacycles was clearly determined by electrospray ionization mass spectrometry (ESI-MS). The main peaks in the ESI mass spectra of (*S*)-**7a** and (S)-**7b** all supported the formation of [3 + 3] triangular structures, including the peak at *m*/*z* = 1390.7892 attributed to [(*S*)-**7a** – 4HOTf – 2OTf + 1K]$^{3+}$ (Figure S15) and the peak at *m*/*z* = 1566.4625 assigned to [(*S*)-**7b** – 2HOTf – 2OTf + 1K]$^{3+}$ (Figure

S20), respectively. These peaks are isotopically resolved and agree very well with their calculated theoretical distributions. No peaks were observed from the self-assemblies with other stoichiometries.

We then used (*S*)-**7a** or (*S*)-**7b** as the catalyst for the asymmetric conjugate addition of chalcone **8a** with *trans*-2-phenylvinylboronic acid **9a**. The preliminary attempt of the reaction in CH_3CN at reflux with 30 mol% $Mg(OtBu)_2$ as the additive (Table 1, Entry 1) showed that (*S*)-**7a** is an effective catalyst for this asymmetric addition to deliver the product **10a** in 38% conversion and 89% ee. The effect of solvent on the reaction was then investigated, which showed that this catalyst system is strongly solvent-dependent. The reaction had almost no activity in DMF (Entry 2) and in dichloromethane (Entry 3), while 50% conversion and 77% ee were achieved in toluene (Entry 4). Considering the catalytic efficiency and the solubility of (*S*)-**7a**, acetonitrile was used as the solvent for further optimization. A variety of magnesium salts, including anhydrous $Mg(OtBu)_2$, $MgSO_4$, $MgCl_2$, $MgBr_2$, and $Mg(OEt)_2$ were screened afterwards (Entries 1 and 5–8). Medium conversions (35–54%) were obtained and the reaction with anhydrous $Mg(OtBu)_2$ gave the highest enantioselectivity (89% ee). Therefore, $Mg(OtBu)_2$ was selected as the final additive.

Table 2. Optimization of other conditions of the asymmetric addition reaction [a]

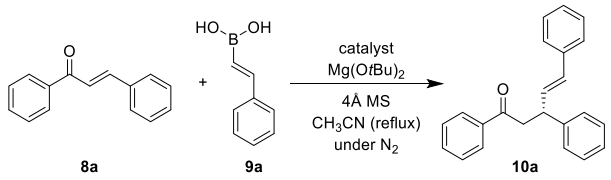

Entry	Catalyst	mol % of $Mg(OtBu)_2$	Time (h)	Conv. (%) [b]	ee (%) [c]
1 [d]	(*S*)-**7a**	30	40	48	91
2	(*S*)-**7a**	30	40	70	90
3	(*S*)-**7a**	45	40	91	94
4	(*S*)-**7a**	67	40	63	93
5	(*S*)-**7a**	0	40	63	91
6 [e]	(*S*)-**7a**	45	40	81	95
7 [f]	(*S*)-**7a**	45	40	75	94
8	(*S*)-**7a**	45	24	46	92
9	(*S*)-**7a**	45	36	82	95
10	(*S*)-**7a**	45	48	90	94
11 [g]	(*S*)-**7a**	45	40	53	54
12 [h]	(*S*)-**7a**	45	40	73	85
13	(*S*)-**7b**	45	40	87	94
14 [i]	(*S*)-**5**	45	40	82	76
15 [j]	(*S*)-**11**	45	40	99	84

[a] Reaction condition: 0.03 mmol **8a**, 0.036 mmol **9a**, 0.0045 mmol catalyst, concentration of **8a** = 0.1 M, 4Å MS (16 mg). [b] Determined by integration of product in ^1H NMR spectra. [c] Determined by HPLC analysis. [d] Concentration of **8a** = 0.08 M. [e] 6 mg 4Å MS. [f] 26 mg 4Å MS. [g] 0.0015 mmol (*S*)-**7a**. [h] 0.003 mmol (*S*)-**7a**. [i] 0.0135 mmol (*S*)-**5**. [j] 0.0135 mmol (*S*)-**11**.

Next, we optimized the concentration of the substrate, the amount of $Mg(OtBu)_2$, the amount of molecular sieve (MS), the reaction time and metalla-triangle catalysts. As shown in Table 2 (Entries 1 and 2), the conversion of **8a** increased from 38% to 70% when the concentration of **8a** increased from 0.05 to 0.1 M (Table 1, Entry 1 *vs* Table 2, Entries 1 and 2). This concentration dependency might be caused by the stronger supramolecular interactions between the reactants and the metallacycle catalyst as their concentrations increased. When the amount of $Mg(OtBu)_2$ increased from 30 mol% to 45 mol%, the addition product **10a** was released in 91% conversion with 94% ee (Table 2, Entry 3). Nonetheless, further enhancement of the amount of $Mg(OtBu)_2$ to 67 mol% (Entry 4) as well as no additive (Entry 5) led to much lower conversions. Entries 3, 6 and 7 showed that the dosage of the molecular sieve could influence the reactivity but not the enantioselectivity. The best ratio was fixed at 16 mg molecular sieve *vs* 0.03 mmol chalcone. We presume that too much additives may reduce the solubility of the reactants and catalyst and affect the molecular collisions although the presence of $Mg(OtBu)_2$ and molecular sieve can accelerate the reaction. The conversion increased from 46% to 91% when the reaction time increased from 24 h to 40 h (Entry 3 *vs* Entries 8 and 9), while further extension of the reaction time to 48 h (Entry 10) did not result in obvious improvement of either conversion or enantioselectivity. A lesser amount of the chiral catalyst (*S*)-**7a** caused significant decreases of both reactivity and enantioselectivity (Entries 11 and 12 *vs* Entry 3). Comparatively, reaction with the larger chiral triangle (*S*)-**7b** as catalyst afforded similar enantioselectivity but slightly lower catalytic ability (Entry 13 *vs* Entry 3), while the BINOL ligand (*S*)-**5** gave only 82% conversion and 76% ee (Entry 14). At the same conditions, the use of 45 mol% (*S*)-3,3'-dibromo-1,1'-bi-2,2'-naphthol ((*S*)-**11**), a superior catalyst previously reported for the asymmetric addition of organoboronates to *α,β*-enones[20a] and the addition of indoles to *α,β*-enones,[20b] provides a quantitative conversion but lower enantioselectivity (84% ee, Entry 15). These results indicate that the catalysts incorporated in the two-dimensional cavity of metallacycles are propitious to the asymmetric reaction.

Scheme 3. Asymmetric conjugate addition of substituted *α,β*-enones and styrylboronic acids catalyzed by (*S*)-7a [a]

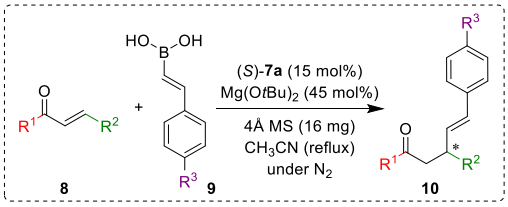

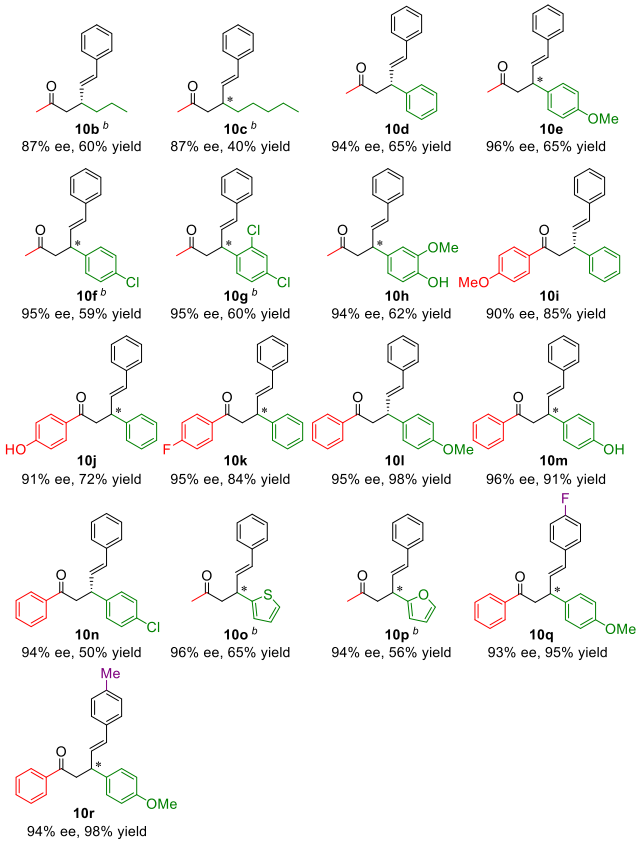

[a] Reaction conditions: 0.03 mmol **8**, 0.036 mmol **9**, 0.0045 mmol (*S*)-**7a**, $Mg(OtBu)_2$ (45 mol%), 4Å MS (16 mg), 0.3 mL acetonitrile, reaction time = 40 h. Isolated yields. The ee values were determined by HPLC analysis. [b] Reaction time = 72 h.

To illustrate the generality of the catalyst system, additions of a series of *α*,*β*-unsaturated ketones were carried out at the optimized conditions (Scheme 3). When R^1 on **8** is methyl, yields of the addition products are lower (40–65%) than the ones with aromatic groups (50–98%). When the R^2 groups are flexible alkyl chains (**8b** and **8c**), medium yields and relatively lower enantioselectivity of 87% ee were achieved, even with longer reaction time (72 h). Nonetheless, addition of the substrates with aromatic or heteroaromatic R^2 groups all gave higher enantioselectivities (94–96% ee for **10d–h**, **10o** and **10p**) regardless of the substituents on the aromatics. For the substituted chalcones, the adducts **10i–n** were obtained in 90–96% ee with up to 98% yields. The *para*-substitution on the phenyl of R^1 with electron-donating groups slightly reduce the enantioselectivity (90% ee for **10i** and 91% ee for **10j**), while the presence of electron-withdrawing group or no substituent on the phenyl of R^1 provide higher enantioselectivities (94–96% ee, **10k–n**). The substituents on the phenyl of R^2 have no obvious effect on the enantioselectivity (**10l–n**); nevertheless, the existence of electron-withdrawing chloride on phenyl of R^2 resulted in a much lower yield of 50% (**10n**). The substituents of R^3 on the phenyl of styrylboronic acid have almost no influence on both the reactivity and enantioselectivity (**10q–r**). The results are significantly better than those (68–88% ee) previously reported on the enantioselective addition of boronic acids to *α*,*β*-enones with similar substrate structures catalyzed by *O*-monoacyltartaric acids[21a] and are comparable to the data (86–98% ee) obtained under the catalysis of an unusual chiral biphenol organocatalyst bearing a complicated tetraphenylene scaffold.[21b]

In summary, we have described the highly efficient construction of two chiral metalla-triangles by coordination-driven self-assembly of a chiral 3,3'-dipyridyl substituted BINOL donor with two 180 °Pt-based acceptors. These two chiral SCCs were characterized by ^1H, $^{31}P\{^1H\}$, and ^1H–^1H COSY NMR, ESI-MS and CD analyses. They were successfully applied in the asymmetric conjugate addition of a wide assortment of *α*,*β*-enones with styrylboronic acids to furnish *γ*,*δ*-unsaturated ketones in 40–98% yields with 87–96% ee. The results showed that the formation of a metallacycle with multiple catalytic sites and suitable chiral cavity is important for the enhancement of activity and stereoselectivity in the reaction. The present studies not only provide convenient pathways to build up new chiral supramolecular macrocycles with interesting structures but also offer an effective strategy for the construction of chiral supramolecular catalysts.

ASSOCIATED CONTENT

Supporting Information

Experimental procedures and analysis data for BINOL derivatives, metallacycles, and asymmetric addition products. This material is available free of charge via the Internet at http://pubs.acs.org.

AUTHOR INFORMATION

Corresponding Author

l_shijun@hznu.edu.cn; stang@chem.utah.edu

Notes

The authors declare no competing financial interest.

ACKNOWLEDGMENT

S.L. thanks the National Natural Science Foundation of China (21773052), the Program for Changjiang Scholars and Innovative Research Team in Chinese University (IRT 1231), and the Program for Social Development of Hangzhou (20170533B10). P.J.S. thanks the NIH (Grant R01 CA215157) for financial support.

REFERENCES

(1) (a) van Leeuwen, P. W. N. M., *Supramolecular Catalysis*; Wiley-VCH, **2008**. (b) Meeuwissen, J.; Reek, J. N. H. Supramolecular Catalysis beyond Enzyme Mimics. *Nature Chem.* **2010**, *2*, 615−621. (c) Wiester, M. J.; Ulmann, P. A.; Mirkin, C. A. Enzyme Mimics Based Upon Supramolecular Coordination Chemistry. *Angew. Chem., Int. Ed.* **2011**, *50*, 114−137. (d) Raynal, M.; Ballester, P.; Vidal-Ferran, A.; van Leeuwen, P. W. N. M. Supramolecular Catalysis. Part 1: Non-covalent Interactions as a Tool for Building and Modifying Homogeneous Catalysts. *Chem. Soc. Rev.* **2014**, *43*, 1660−1733. (e) Raynal, M.; Ballester, P.; Vidal-Ferran, A.; van Leeuwen, P. W. N. M. Supramolecular Catalysis. Part 2: Artificial Enzyme Mimics. *Chem. Soc. Rev.* **2014**, *43*, 1734−1787. (f) Brown, C. J.; Toste, F. D.; Bergman, R. G.; Raymond, K. N. Supramolecular Catalysis in Metal–Ligand Cluster Hosts. *Chem. Rev.* **2015**, *115*, 3012−3035. (g) Gao, W.-X.; Zhang, H.-N.; Jin, G.-X. Supramolecular Catalysis Based on Discrete Heterometallic Coordination-Driven Metallacycles and Metallacages. *Coord. Chem. Rev.* **2019**, *386*, 69−84.

(2) (a) Breit, B. Supramolecular Approaches to Generate Libraries of Chelating Bidentate Ligands for Homogeneous Catalysis. *Angew. Chem., Int. Ed.* **2005**, *44*, 6816−6825. (b) Ma, L.; Abney, C.; Lin, W. Enantioselective Catalysis with Homochiral Metal–Organic Frameworks. *Chem. Soc. Rev.* **2009**, *38*, 1248−1256. (c) Dong, Z.; Luo, Q.; Liu, J. Artificial Enzymes Based on Supramolecular Scaffolds. *Chem. Soc. Rev.* **2012**, *41*, 7890−7908. (d) Leenders, S. H. A. M.; Gramage-Doria, R.; de Bruin, B.; Reek, J. N. H. Transition Metal Catalysis in Confined Spaces. *Chem. Soc. Rev.* **2015**, *44*, 433−448. (e) Vaquero, M.; Rovira, L.; Vidal-Ferran, A. Supramolecularly Fine-Regulated Enantioselective Catalysts. *Chem. Commun.* **2016**, *52*, 11038−11051. (f) Nurttila, S. S.; Linnebank, P. R.; Krachko, T.; Reek, J. N. H. Supramolecular Approaches To Control Activity and Selectivity in Hydroformylation Catalysis. *ACS Catal.* **2018**, *8*, 3469−3488.

(3) (a) Hapiot, F.; Bricout, H.; Menuel, S.; Tilloy, S.; Monflier, E. Recent Breakthroughs in Aqueous Cyclodextrin-Assisted Supramolecular Catalysis. *Catal. Sci. Technol.* **2014**, *4*, 1899−1908. (b) Ouyang, G.-H.; He, Y.-M.; Fan, Q.-H. Podand-Based Dimeric Chromium(III)-Salen Complex

for Asymmetric Henry Reaction: Cooperative Catalysis Promoted by Complexation of Alkali Metal Ions. *Chem. Eur. J.* **2014**, *20*, 16454−16457. (c) Ouyang, G.-H.; He, Y.-M.; Li, Y.; Xiang, J.-F.; Fan, Q.-H. Cation-Triggered Switchable Asymmetric Catalysis with Chiral Aza-CrownPhos. *Angew. Chem., Int. Ed.* **2015**, *54*, 4334–4337. (d) Vidal-Ferran, A.; Mon, I.; Bauzá, A.; Frontera, A.; Rovira, L. Supramolecularly Regulated Ligands for Asymmetric Hydroformylations and Hydrogenations. *Chem. Eur. J.* **2015**, *21*, 11417−11426. (e) Zhang, X.-C.; Hu, Y.-H.; Chen, C.-F.; Fang, Q.; Yang, L.-Y.; Lu, Y.-B.; Xie, L.-J.; Wu, J.; Li, S.; Fang, W. A Supramolecularly Tunable Chiral Diphosphine Ligand: Application to Rh and Ir-catalyzed Enantioselective Hydrogenation. *Chem. Sci.* **2016**, *7*, 4594−4599. (f) Jiao, Y.; Tang, B.; Zhang, Y.; Xu, J.-F.; Wang, Z.; Zhang, X. Highly Efficient Supramolecular Catalysis by Endowing the Reaction Intermediate with Adaptive Reactivity. *Angew. Chem., Int. Ed.* **2018**, *57*, 6077−6081.

(4) (a) Kaphan, D. M.; Levin, M. D.; Bergman, R. G.; Raymond, K. N.; Toste, F. D. A Supramolecular Microenvironment Strategy for Transition Metal Catalysis. *Science* **2015**, *350*, 1235−1238. (b) Wang, Q.-Q.; Gonell, S.; Leenders, S. H. A. M.; Dürr, M.; Ivanović-Burmazović, I.; Reek, J. N. H. Self-Assembled Nanospheres with Multiple Endohedral Binding Sites Pre-Organize Catalysts and Substrates for Highly Efficient Reactions. *Nature Chem.* **2016**, *8*, 225−230. (c) Guo, J.; Xu, Y.-W.; Li, K.; Xiao, L.-M.; Chen, S.; Wu, K.; Chen, X.-D.; Fan, Y.-Z.; Liu, J.-M.; Su, C.-Y. Regio- and Enantioselective Photodimerization within the Confined Space of a Homochiral Ruthenium/Palladium Heterometallic Coordination Cage. *Angew. Chem., Int. Ed.* **2017**, *56*, 3852−3856. (d) Tan, C.; Jiao, J.; Li, Z.; Liu, Y.; Han, X.; Cui, Y. Design and Assembly of a Chiral Metallosalen-Based Octahedral Coordination Cage for Supramolecular Asymmetric Catalysis. *Angew. Chem., Int. Ed.* **2018**, *57*, 2085−2090. (e) Tan, C.; Chu, D.; Tang, X.; Liu, Y.; Xuan, W.; Cui, Y. Supramolecular Coordination Cages for Asymmetric Catalysis. *Chem. Eur. J.* **2019**, *25*, 662−672. (f) Li, X.; Wu, J.; He, C.; Meng, Q.; Duan, C. Asymmetric Catalysis within the Chiral Confined Space of Metal–Organic Architectures. *Small* **2019**, *15*, 1804770.

(5) (a) Park, J.; Lang, K.; Abboud, K. A.; Hong, S. Self-Assembled Dinuclear Cobalt(II)-Salen Catalyst Through Hydrogen-Bonding and Its Application to Enantioselective Nitro-Aldol (Henry) Reaction. *J. Am. Chem. Soc.* **2008**, *130*, 16484−16485. (b) Wieland, J.; Breit, B. A Combinatorial Approach to the Identification of Self-Assembled Ligands for Rhodium-Catalysed Asymmetric Hydrogenation. *Nature Chem.* **2010**, *2*, 832–837. (c) Mote, N. R.; Chikkali, S. H. Hydrogen-Bonding-Assisted Supramolecular Metal Catalysis. *Chem. Asian J.* **2018**, *13*, 3623−3646.

(6) (a) Howlader, P.; Das, P.; Zangrando, E.; Mukherjee, P. S. Urea-Functionalized Self-Assembled Molecular Prism for Heterogeneous Catalysis in Water. *J. Am. Chem. Soc.* **2016**, *138*, 1668−1676. (b) Bräuer, T. M.; Zhang, Q.; Tiefenbacher, K. Iminium Catalysis inside a Self-Assembled Supramolecular Capsule: Scope and Mechanistic Studies. *J. Am. Chem. Soc.* **2017**, *139*, 17500−17507.

(7) (a) Leininger, S.; Olenyuk, B.; Stang, P. J. Self-Assembly of Discrete Cyclic Nanostructures Mediated by Transition Metals. *Chem. Rev.* **2000**, *100*, 853−908. (b) Fujita, M.; Tominaga, M.; Hori, A.; Therrien, B. Coordination Assemblies from a Pd(II)-Cornered Square Complex. *Acc. Chem. Res.* **2005**, *38*, 369−378. (c) Eryazici, I.; Moorefield, C. N.; Newkome, G. R. Square-planar Pd(II), Pt(II), and Au(III) Terpyridine Complexes: Their Syntheses, Physical Properties, Supramolecular Constructs, and Tiomedical Activities. *Chem. Rev.* **2008**, *108*, 1834−1895. (d) Yoshizawa, M.; Klosterman, J. K.; Fujita, M. Functional Molecular Flasks: New Properties and Reactions within Discrete, Self-Assembled Hosts. *Angew. Chem., Int. Ed.* **2009**, *48*, 3418−3438. (e) Chakrabarty, R.; Mukherjee, P. S.; Stang, P. J. Supramolecular Coordination: Self-Assembly of Finite Two- and Three-Dimensional Ensembles. *Chem. Rev.* **2011**, *111*, 6810−6918. (f) Cook, T. R.; Stang, P. J. Recent Developments in the Preparation and Chemistry of Metallacycles and Metallacages via Coordination. *Chem. Rev.* **2015**, *115*, 7001−7045. (g) Zhang, D.; Ronson, T. K.; Nitschke, J. R. Functional Capsules via Subcomponent Self-Assembly. *Acc. Chem. Res.* **2018**, *51*, 2423−2436. (h) Wu, G.-Y.; Chen, L.-J.; Xu, L.; Zhao, X.-L.; Yang, H.-B. Construction of Supramolecular Hexagonal Metallacycles via Coordination-Driven Self-Assembly: Structure, Properties and Application. *Coord. Chem. Rev.* **2018**, *369*, 39−75. (i) Sun, Y.; Chen, C.; Stang, P. J. Soft Materials with Diverse Suprastructures via the Self-Assembly of Metal−Organic Complexes. *Acc. Chem. Res.* **2019**, *52*, 802−817.

(8) (a) Yan, X.; Wang, H.; Hauke, C. E.; Cook, T. R.; Wang, M.; Saha, M. L.; Zhou, Z.; Zhang, M.; Li, X.; Huang, F.; Stang, P. J. A Suite of Tetraphenylethylene-Based Discrete Organoplatinum(II) Metallacycles: Controllable Structure and Stoichiometry, Aggregation-Induced Emission, and Nitroaromatics Sensing. *J. Am. Chem. Soc.* **2015**, *137*, 15276−15286. (b) Zhang, Z.; Zhao, Z.; Wu, L.; Lu, S.; Ling, S.; Li, G.; Xu, L.; Ma, L.; Hou, Y.; Wang, X.; Li, X.; He, G.; Wang, K.; Zou, B.; Zhang, M. Emissive Platinum(II) Cages with Reverse Fluorescence Resonance Energy Transfer for Multiple Sensing. *J. Am. Chem. Soc.* **2020**, *142*, 2592−2600.

(9) (a) Li, S.; Huang, J.; Cook, T. R.; Pollock, J. B.; Kim, H.; Chi, K.-W.; Stang, P. J. Formation of [3]Catenanes from 10 Precursors via Multi-Component Coordination-Driven Self-Assembly of Metallarectangles. *J. Am. Chem. Soc.* **2013**, *135*, 2084−2087. (b) Lin, W.; Cen, T.-Y.; Wang, S.-P.; Zhang, Z.; Wu, J.; Huang, J.; Li, S. Anion Recognition with Porphyrin-bottomed Tetraurea Receptors. *Chin. Chem. Lett.* **2018**, *29*, 1372−1374. (c) Shi, B.; Zhou, Z.; Vanderlinden, R. T.; Tang, J.-H.; Yu, G.; Acharyya, K.; Sepehrpour, H.; Stang, P. J. Spontaneous Supramolecular Polymerization Driven by Discrete Platinum Metallacycle-Based Host–Guest Complexation. *J. Am. Chem. Soc.* **2019**, *141*, 11837−11841. (d) Saha, R.; Devaraj, A.; Bhattacharyya, S.; Das, S.; Zangrando, E.; Mukherjee, P. S. Unusual Behavior of Donor−Acceptor Stenhouse Adducts in Confined Space of a Water-Soluble Pd^{II}_8 Molecular Vessel. *J. Am. Chem. Soc.* **2019**, *141*, 8638−8645. (e) Rizzuto, F. J.; von Krbek, L. K. S.; Nitschke, J. R. Strategies for Binding Multiple Guests in Metal–Organic Cages. *Nat. Rev. Chem.* **2019**, *3*, 204−222.

(10) Yan, K. K.; Dubey, R.; Arai, T.; Inokuma, Y.; Fujita, M. Chiral Crystalline Sponges for the Absolute Structure Determination of Chiral Guests. *J. Am. Chem. Soc.* **2017**, *139*, 11341−11344.

(11) Acharyya, K.; Bhattacharyya, S.; Sepehrpour, H.; Chakraborty, S.; Lu, S.; Shi, B.; Li, X.; Mukherjee, P. S.; Stang, P. J. Self-Assembled Fluorescent Pt(II) Metallacycles as Artificial Light-Harvesting Systems. *J. Am. Chem. Soc.* **2019**, *141*, 14565−14569.

(12) Zhang, D.; Ronson, T. K.; Lavendomme, R.; Nitschke, J. R. Selective Separation of Polyaromatic Hydrocarbons by Phase Transfer of Coordination Cages. *J. Am. Chem. Soc.* **2019**, *141*, 18949−18953.

(13) Chen, L.-J.; Yang, H.-B. Construction of Stimuli-Responsive Functional Materials via Hierarchical Self-Assembly Involving Coordination Interactions. *Acc. Chem. Res.* **2018**, *51*, 2699−2710.

(14) (a) Cook, T. R.; Vajpayee, V.; Lee, M. H.; Stang, P. J.; Chi, K.-W. Biomedical and Biochemical Applications of Self-Assembled Metallacycles and Metallacages. *Acc. Chem. Res.* **2013**, *46*, 2464−2474. (b) Yu, G.; Zhu, B.; Shao, L.; Zhou, J.; Saha, M. L.; Shi, B.; Zhang, Z.; Hong, T.; Li, S.; Chen, X.; Stang, P. J. Host-guest Complexation-Mediated Codelivery of Anticancer Drug and Photosensitizer for Cancer Photochemotherapy. *Proc. Natl. Acad. Sci. USA* **2019**, *116*, 6618−6623. (c) Qin, Y.; Chen, L.-J.; Dong, F.; Jiang, S.-T.; Yin, G.-Q.; Li, X.; Tian, Y. Yang, H.-B. Light-Controlled Generation of Singlet Oxygen within a Discrete Dual-Stage Metallacycle for Cancer Therapy. *J. Am. Chem. Soc.* **2019**, *141*, 8943−8950. (d) Sepehrpour, H.; Fu, W.; Sun, Y.; Stang, P. J. Biomedically Relevant Self-Assembled Metallacycles and Metallacages. *J. Am. Chem. Soc.* **2019**, *141*, 14005−14020.

(15) (a) Lee, S. J.; Lin, W. A Chiral Molecular Square with Metallo-Corners for Enantioselective Sensing. *J. Am. Chem. Soc.* **2002**, *124*, 4554−4555. (b) Gütz, C.; Hovorka, R.; Klein, C.; Jiang, Q. Q.; Bannwarth, C.; Engeser, M.; Schmuck, C.; Assenmacher, W.; Mader, W.; Topić, F.; Rissanen, K.; Grimme, S.; Lützen, A. Enantiomerically Pure $[M_6L_{12}]$ or $[M_{12}L_{24}]$ Polyhedra from Flexible Bis(Pyridine) Ligands. *Angew. Chem., Int. Ed.* **2014**, *53*, 1693−1698. (c) Chen, L.-J.; Yang, H.-B.; Shionoya, M. Chiral Metallosupramolecular Architectures. *Chem. Soc. Rev.* **2017**, *46*, 2555−2576. (d) Pan, M.; Wu, K.; Zhang, J.-H.; Su, C.-Y. Chiral Metal–Organic Cages/Containers (MOCs): From Structural and Stereochemical Design to Applications. *Coord. Chem. Rev.* **2019**, *378*, 333−349.

(16) (a) Stang, P. J.; Olenyuk, B. Directed Self-Assembly of Chiral, Optically Active Macrocyclic Tetranuclear Molecular Squares. *Angew. Chem., Int. Ed.* **1996**, *35*, 732−736. (b) Lee, S. J.; Hu, A.; Lin, W. The First Chiral Organometallic Triangle for Asymmetric Catalysis. *J. Am. Chem. Soc.* **2002**, *124*, 12948−12949. (c) Ou-Yang, J.-K.; Zhang, Y.-Y.; He, M.-L.; Li, J.-T.; Li, X.; Zhao, X.-L.; Wang, C.-H.; Yu, Y.; Wang, D.-X.; Xu, L.; Yang, H.-B. Unexpected Self-Assembly of Chiral Triangles from 90 °Chiral DiPt(II) Acceptors. *Org. Lett.* **2014**, *16*, 664−667. (d) Ye, Y.; Cook, T. R.; Wang, S.-P.; Wu, J.; Li, S.; Stang, P. J. Self-Assembly of Chiral Metallacycles and Metallacages from a Directionally Adaptable BINOL-Derived Donor. *J. Am. Chem. Soc.* **2015**, *137*, 11896−11899. (e) Bhat, I. A.; Devaraj, A.; Howlader, P.; Chi, K.-W.; Mukherjee, P. S. Preparation of a Chiral Pt_{12} Tetrahedral Cage and its Use in Catalytic Michael Addition Reaction. *Chem. Commun.* **2018**, *54*, 4814−4817.

(17) Noyori, R.; Tomino, I.; Tanimoto, Y. Virtually Complete Enantioface Differentiation in Carbonyl Group Reduction by a Complex Aluminum Hydride Reagent. *J. Am. Chem. Soc.* **1979**, *101*, 3129−3131.

(18) (a) Brunel, J. M. BINOL: A Versatile Chiral Reagent. *Chem. Rev.* **2005**, *105*, 857−897. (b) Parmar, D.; Sugiono, E.; Raja, S.; Rueping, M. Complete Field Guide to Asymmetric BINOL-Phosphate Derived Bronsted Acid and Metal Catalysis: History and Classification by Mode of Activation; Bronsted Acidity, Hydrogen Bonding, Ion Pairing, and Metal Phosphates. *Chem. Rev.* **2014**, *114*, 9047−9153.

(19) (a) Lou, S.; Moquist, P. N.; Schaus, S. E. Asymmetric Allylboration of Ketones Catalyzed by Chiral Diols. *J. Am. Chem. Soc.* **2006**, *128*, 12660−12661. (b) Lin, L.; Zhang, J.; Ma, X.; Fu, X.; Wang, R. Bifunctional 3,3'-Ph_2-BINOL-Mg Catalyzed Direct Asymmetric Vinylogous Michael Addition of *α,β*-Unsaturated *γ*-Butyrolactam. *Org. Lett.* **2011**, *13*, 6410−6413. (c) Le, P. Q.; Nguyen, T. S.; May, J. A. A General Method for the Enantioselective Synthesis of *α*-Chiral Heterocycles. *Org. Lett.* **2012**, *14*, 6104−6107. (c) Jiang, Y.; Schaus, S. E. Asymmetric Petasis Borono-Mannich Allylation Reactions Catalyzed by Chiral Biphenols. *Angew. Chem., Int. Ed.* **2017**, *56*, 1544−1548. (d) Han, Y.-Q.; Ding, Y.; Zhou, T.; Yan, S.-Y.; Song, H.; Shi, B.-F. Pd(II)-Catalyzed Enantioselective Alkynylation of Unbiased Methylene C(sp^3)−H Bonds Using 3,3′-Fluorinated-BINOL as a Chiral Ligand. *J. Am. Chem. Soc.* **2019**, *141*, 4558−4563.

(20) (a) Wu, T. R.; Chong, J. M. Asymmetric Conjugate Alkenylation of Enones Catalyzed by Chiral Diols. *J. Am. Chem. Soc.* **2007**, *129*, 4908−4909. (b) Blay, G.; Fernández, I.; Pedro, J. R.; Vila, C. Highly Enantioselective Friedel-Crafts Alkylations of Indoles with Simple Enones Catalyzed by Zirconium(IV)-BINOL Complexes. *Org. Lett.* **2007**, *9*, 2601−2604.

(21) (a) Sugiura, M.; Tokudomi, M.; Nakajima, M. Enantioselective Conjugate Addition of Boronic Acids to Enones Catalyzed by O-Monoacyltartaric Acids. *Chem. Commun.* **2010**, *46*, 7799−7800. (b) Chai, G.-L.; Sun, A.-Q.; Zhai, D.; Wang, J.; Deng, W.-Q.; Wong, H. N. C.; Chang, J. Chiral Hydroxytetraphenylene-Catalyzed Asymmetric Conjugate Addition of Boronic Acids to Enones. *Org. Lett.* **2019**, *21*, 5040−5045.

TOC Graphic:

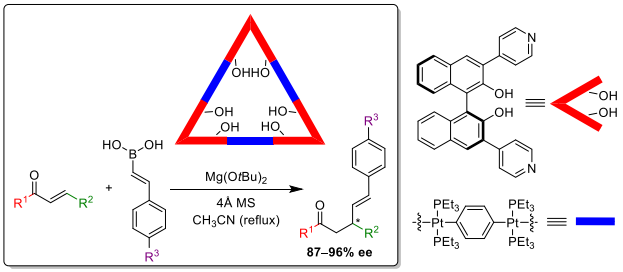
OHHO
OH
OH
HO
HO
HO
B
OH
R3
R1
R2
Mg(OtBu)2
4Å MS
CH3CN (reflux)
87–96% ee
N
OH
OH
OH
OH
N
PEt3
PEt3
Pt
Pt
PEt3
PEt3